Behaviour of the spinning gyro rotor

BEHAVIOUR OF THE SPINNING GYRO ROTOR

by

Ir. C. Huber

Group Measurement and Control
Department of Electrical Engineering
Eindhoven University of Technology
Eindhoven, The Netherlands

BEHAVIOUR OF THE SPINNING GYRO ROTOR

BY

Ir. C. Huber

TH-Report 73-E-34

February 1973

ISBN 90 6144 034 3

Abstract

An elementary understanding of the physical laws governing the spinning rotor is necessary to grasp the essence and function of the various gyroscopic instruments found in to-day's aerospace and maritime vehicle control systems. This report gives a brief exhibition of the very basic phenomena of gyro behaviour in a way that may especially appeal to the control engineer with a limited educational background in the field of mechanical engineering.

Contents

BEHAVIOUR OF THE SPINNING GYRO ROTOR

Ir. C. Huber
Eindhoven University of Technology
Department of Electrical Engineering
Eindhoven, Netherlands

1. Introduction

The rigidity of the rotation axis of a spinning body is a remarkable phenomenon. It invariably puzzles those confronted with it for the first time. But, though the complete theoretical treatment of spinning bodies belongs to the advanced subjects in mechanics (e.g. DEIMEL, MAGNUS)*, the basic principle involved appears to be of beautiful simplicity.

The spinning motion is built up by torques applied during lengths of time. Torques can be regarded as vector quantities, and the time integral of a torque applied to a freely rotatable rigid body becomes the angular momentum of that body. The history of all torque vectors ever applied to the body is summed up in the momentary angular momentum, which too is a vector quantity.

If no further torque is applied to the body it will retain it's angular momentum's magnitude and direction indefinitely, and nothing but a torque applied during some time will ever change it. If we can manage to keep a spinning body free of torques we can use its angular momentum vector as a directional reference with respect to inertial space.
It is this basic property of a spinning body that has led man to make use of such in solving a wide range of inertial rotation measurement and vehicle control problems.

---

* See list of references on page 16.

Gyros used in the presence of gravity or other accelerations have to have a rotor suspension. The most widely used device for this purpose is the Cardanic gimbal system.

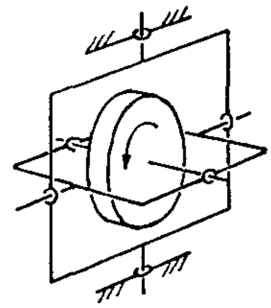

Fig. 1.-1. Cardanic gimbal suspension.

The present paper, however, is not concerned with such practical aspects as how to realize certain conditions or requirements. Consequently, only idealized concepts shall be used here, such as infinite rigidity, zero impedance, rotor floating in space, etc. But it is this radical idealisation of concepts that frees us from the burden of approximations and makes the basic reasoning simple.

2. Theory of gyro behaviour

It is easy to gain insight into the elementary behaviour of the spinning rotor by dividing the subject into two separate aspects:

a. Behaviour of the angular momentum VECTOR in space (steady state kinematics),
b. Behaviour of the gyroscope viewed as mechanical two-port (transient state dynamics).

A rigid body always has three principal axes of inertia (MAGNUS, SAVET). Usually the rotor of a gyro has the semblance of a wheel, and for our considerations we shall assume such a wheel for the which the three principal moments of inertia show this relationship:

$$J_1 = J_2 < J_3 \qquad 2.-(1)$$

Rotation shall be around the axis of J_3 (see fig. 2.1.-1.). This is a stable condition (MAGNUS, p.75).

This spinning rotor will be assumed to be floating in space. As a gyro it is characterized by the product of J_3 and its rotation speed vector $\bar{\omega}_3$, which product is the angular momentum vector

$$\bar{b} = \bar{\omega}_3 . J_3 \qquad 2.-(2)$$

2.1. Steady state behaviour

Let the spinning rotor be represented by the following figure:

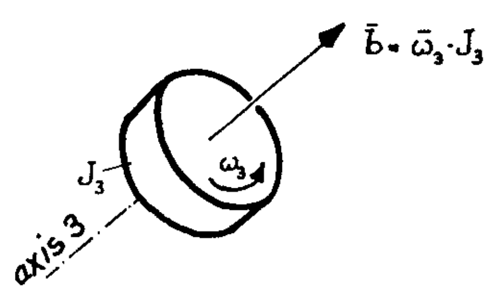

Fig. 2.1.-1. The spinning rotor.
The axes of J_1 and J_2 are orthogonal to each other and to the axis of J_3, which is also the spin axis.

Generation of the angular momentum

The angular momentum is generated by applying a torque $\bar{T}$ to the axis 3 during some length of time:

$$\bar{b} = \bar{\omega}_3 . J_3 = \int \bar{T}_{(3)} dt \qquad 2.1.-(1)$$

The angular momentum can be regarded as the result of a torque-pulse, quite in analogy to magnitudes generated by pulses of other dimension, e.g.:

linear momentum $\bar{P} = \bar{v}.M = \int \bar{F}dt$,
electric charge $Q = U.C = \int Idt$

Conservation of momentum

Differentiation of eq. 2.1.-(1) yields

$$\frac{d\bar{b}}{dt} = \bar{T} \qquad 2.1.-(2)$$

This means that the angular momentum $\bar{b}$ can only be changed by a torque $\bar{T}$. As long as $\bar{T} = 0$ the momentum vector $\bar{b}$ will remain constant. This phenomenon is referred to as the conservation of angular momentum with the absence of torques.

Momentum change with arbitrary torque

The modulus as well as the orientation of a vector can only be altered by adding to it a vector of the same dimensionality. According to eq. 2.1.-(1) $\bar{T}dt$ is such a vector belonging to $\bar{b}$:

$$\overline{db} = \bar{T}dt \qquad 2.1.-(3)$$

A change of the momentum vector $\bar{b}$ can never be effected "suddenly". The torque $\bar{T}$ has always to be applied during some length of time, and the change always is in the direction of $\bar{T}$.
This is illustrated by the following diagram:

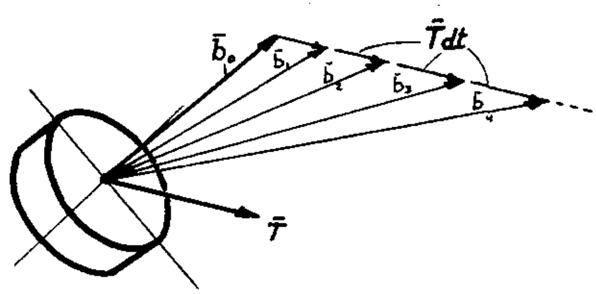

Fig. 2.1.-2. Changing the momentum vector $\bar{b}$ by appling a torque $\bar{T}$.

The orientation of $\bar{T}$ with respect to $\bar{b}_o$, in fig. 2.1.-2., is such that the angular momentum vector changes its length as well as its direction. Thus the rotor will increase its speed of rotation (around axis 3, see fig. 2.1.-1.), and the torque generator not only delivers a torque, but energy to the rotor. The energy accumulated in the rotor is

$$E = (J_3 . \omega_3^2)/2 = \int (\bar{T} . \bar{\omega}_3) dt \qquad 2.1.-(4)$$

and the power required to speed up the rotor is

$$P = \dot{E} = (\bar{T} . \bar{\omega}) \qquad 2.1.-(5)$$

Power-free change of momentum

It is also possible to change the angular momentum vector without delivering energy to the rotor, i.e. without speeding it up. This happens when the torque vector $\bar{T}$ is constantly kept at right angles to the momentum vector $\bar{b}$. Graphically interpreted the point of the vector $\bar{b}$ then follows a bow of a circle, see fig. 2.1.-3.

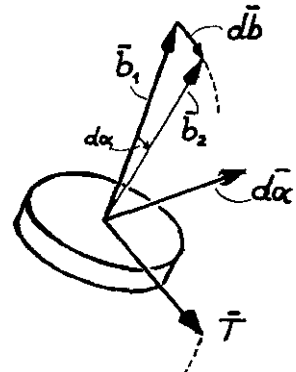

Fig. 2.1.-3. The circular path described by the point of $\bar{b}$ when the momentum is changed power-free. The vector $\bar{b}$ has been given the indices 1 and 2 to show the chronological sequence.

The angular velocity of the sweeping vector $\bar{b}$ can easily be derived from the geometry of fig. 2.1.-3., namely

$$d\alpha = \frac{db}{b} = \frac{Tdt}{b} , \qquad 2.1.-(6)$$

thus for the angular rate

$$\dot{\alpha} = \frac{d\alpha}{dt} = \frac{T}{b} . \qquad 2.1.-(7)$$

Note that this derivation of $\dot{\alpha} = f(T)$ requires the employment of the moduli of the vector quantities, since division of vectors is not uniquely defined. However, here we are dealing with the vectors $\bar{T}$ and $\bar{b}$ orthogonally oriented to each other, and we can easily conclude from fig. 2.1.-3. that $\dot{\alpha}$ as a vector (thus $\bar{\dot{\alpha}}$) is perpendicular to both $\bar{T}$ and $\bar{b}$. The use of the moduli in this case is therefore permissible.

Rigidity of the gyro

From fig. 2.1.-3. one can easily deduce how it comes that a gyro with a larger momentum $\bar{b}$ is more "rigid" than a gyro with a smaller $\bar{b}$. For, with the same torque $\bar{T}$ and the same time increment dt the momentum change $\bar{T}dt = d\bar{b}$ will produce a smaller angular increment $d\bar{\alpha}$ the larger $\bar{b}$ becomes.

Gyro in gimbals

Suppose we have a spinning rotor suspended by two gimbals as depicted in fig. 1.-1. Assume the spin axis bearings to be free of friction. It will then be impossible to exert any torques in the direction of the spin axis by turning the gimbals. In other words, it will be impossible to change the magnitude of the momentum by means of the gimbals. Of any torque applied to the gimbal system only a component orthogonal to the momentary spin axis can be transmitted (disregarding transient phenomena, which are to be treated in the succeeding chapter). Any change of the orientation of the spin axis therefore will be effected free of power.

In this situation, a torque that rotates along with the moving gimbal results in a constant precession rate of the spin axis. With a torque that remains constant in space, however, the spin axis will merely turn until all torque components perpendicular to the spin axis have vanished. Then the momentum vector $\bar{b}$ will have aligned itself with the torque vector $\bar{T}$.

2.2. Dynamic behaviour.

In order to study the dynamic behaviour we shall make a few practical assumptions. The first is that the rotor be spinning at a constant speed and that torques applied never change that speed, but only the direction of the angular momentum vector in the power-free manner described in chapter 2.1. The torque vector $\bar{T}$ thus must always be at right angles to the momentum vector $\bar{b}$. From fig. 2.1.-3. we learn that the precession rate vector $\bar{\dot{\alpha}}$ must always be at right angles to both $\bar{T}$ and $\bar{b}$. We thus have an orthogonal system in which

$$\bar{\dot{\alpha}} \times \bar{b} = \bar{T}. \qquad 2.2.-(1)$$

The second assumption is that we consider both $\bar{T}$ and $\bar{\dot{\alpha}}$ to have a fixed direction in inertial space as long as we are dealing with transient responses only. This we may do as long as we can neglect the small transient angular excursions $\Delta\alpha$ with respect to the steady state direction of $\bar{b}$.

These two assumptions mean that we are dealing with an orthogonal setup at all times, and that we can drop the vector notations for T, b, and $\dot{\alpha}$. We know the directions of T and $\dot{\alpha}$, and we define them as input and output axes. In general, when we apply a torque to the input axis we can expect some angular movement. Thus the input magnitudes become T_1 and $\dot{\alpha}_1$. In analogy to this the output axis will, in general, be able to exert a torque when moving, so the output pair becomes T_2 and α_2. Both axes are geometrically decoupled due to their orthogonality, and if we assume the rotor to be floating in space to avoid suspension problems we can imagine it caught in a system of forks as is shown in fig. 2.2.-1.

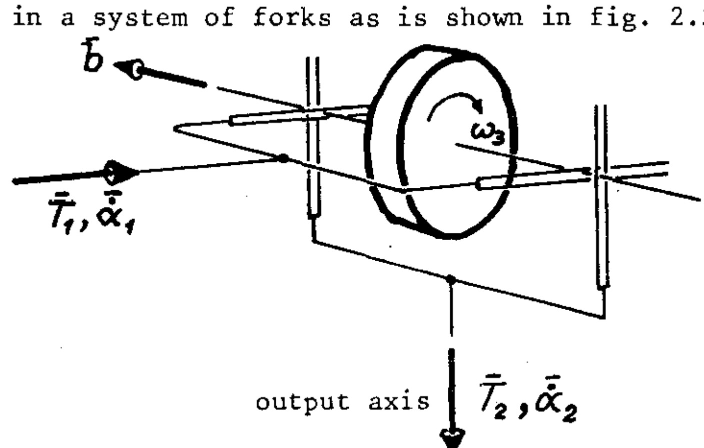

Fig. 2.2.-1. The gyro as a mechanical two-port.

As long as the rotor is not spinning, turning one fork will not influence the other, but when the rotor is sped up the two forks will be coupled with each other on the basis of the mechanical laws governing spinning bodies. The arrangement can be regarded as a mechanical two-port, and we shall analyze its behaviour as such, assuming the angular excursions of the two guiding forks as very small.

One-ports and two-ports

Let a one-port ($\hat{=}$ two-pole) in an arbitrary system (electrical, mechanical rectilinear, mechanical rotatory, magnetical, etc.) be characterized by two state variables (voltage - current; force - velocity; torque - angular rate magnetomotoric force - flux rate;etc.)having a specific relation to each other at that port (e.g. voltage per unit current = impedance).

In such a system a two-port (≙ four-pole) is characterized by the relation between the state variables at the input and output port. A transducer is a two-port of special interest to us. With the ideal transducer a relationship exists between one of each state variables at the input and one of those at the output, but not mutually between the two state variables at either input or output. The ideal transducer is able to transmit each input state variable to the output independantly from the other.

Iterative matrices of ideal transducers

The iterative matrix of an ideal transducer shows the transduction coefficient and its reciprocal in one of the diagonals, whereas the other diagonal contains only zeroes:

$$\begin{Vmatrix} \alpha & 0 \\ 0 & \frac{1}{\alpha} \end{Vmatrix} \quad \text{or} \quad \begin{Vmatrix} 0 & \beta \\ \frac{1}{\beta} & 0 \end{Vmatrix} \qquad 2.2.-(2)$$

The ideal transformer is an electrical example for the transformatoric type of transducer (see lefthand matrix in 2.2.-(2)) whereas a spinning rotor according to fig. 2.2.-1. with some idealisations forms an example of the gyratoric transducer (see other matrix in 2.2.-(2)).

The gyro as an ideal transducer

From eq. 2.2.-(1) we can conclude that with the gyro the two state variables involved are $\bar{\dot{\alpha}}$ and $\bar{T}$. We have assigned fixed directions to these vector variables according to fig. 2.2.-1. Forthwith we shall be merely interested in the time-functions of the moduli $\dot{\alpha}$ and T.

We have thus arrived at a mechanical two-port the equations of which can be written as

$$\left.\begin{aligned} T_1 &= 0.T_2 + b\dot{\alpha}_2 \\ \dot{\alpha}_1 &= \frac{1}{b}.T_2 + 0.\dot{\alpha}_2 \end{aligned}\right\} \quad 2.2.-(3)$$

The matrix-form of 2.2.-3 is

$$\begin{pmatrix} T_1 \\ \dot{\alpha}_1 \end{pmatrix} = \begin{pmatrix} 0 & b \\ \frac{1}{b} & 0 \end{pmatrix} \cdot \begin{pmatrix} T_2 \\ \dot{\alpha}_2 \end{pmatrix} \qquad 2.2.-(4)$$

and the appertaining two-port will be:

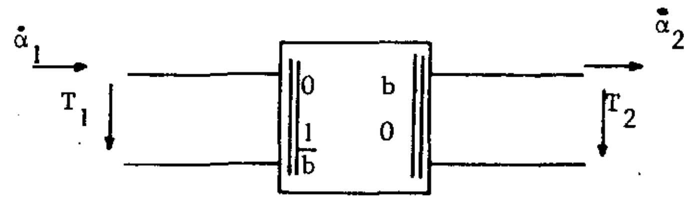

Fig. 2.2.-2. The two-port equivalent of the idealized gyro.

The transduction factor is $b=\omega_3.J_3$ (compare eq. 2.-(2)). In analogy to this the electrical Hall-effect gyrator's transduction factor h is the product of the magnetic induction and the Hall-constant, namely h = B.k. The Hall-constant k of the material used can be compared with the moment of inertia J_3, whereas the speed of rotation ω_3 represents a kind of biasing, or rather energizing, just as the induction B does. Both constituents of the transduction factor, in each case, together lend the proper physical dimension to the transduction factor.

Just as the ideal transformer does not exist in the physcial realm, so the idealized gyratoric two-port as represented by eq. 2.2.-(4) is an abstracted circuit element. The ideal transformer is approximated when the copper losses, stray inductances and the admittance of the main inductivity become negligibly small. In order to arrive at an ideal circuit element from a gyro according to fig. 2.2.-1 the forks would have to become infinitely rigid and massless, the friction with the axle would have to approach zero. Then, if $\omega_3 \to \infty$ and $J_3 \to 0$ simultaneously, the angular momentum $b = \omega_3.J_3$ can retain its finite value just as the ratio of the windings of a transformer can do even though the total number of windings may grow very large.

Introducing disturbing elements

However, any practical gyro will be encumbered by disturbing elements. The most conspicuous ones will be the moments of inertia J_1 and J_2 (see explanation below fig. 2.1.-1.). One can regard them as oriented along the input and output axes of the two-port, fig. 2.2.-1. The fork or gimbal inertia has to be added, and if we think of them as comprised in J_1 and J_2 we can draw the following schematic:

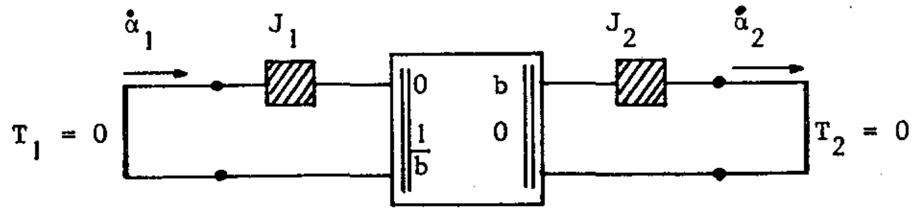

Fig. 2.2.-3. The moments of inertia J_1 and J_2 added to the ideal gyro two-port.

The "short-circuited" input and output indicate that both the input and output axes are free of external torques, or so to say freewheeling, unburdened.

Applying a signal source

The input short-circuit can be replaced by a torque generator as in fig. 2.2.-4.:

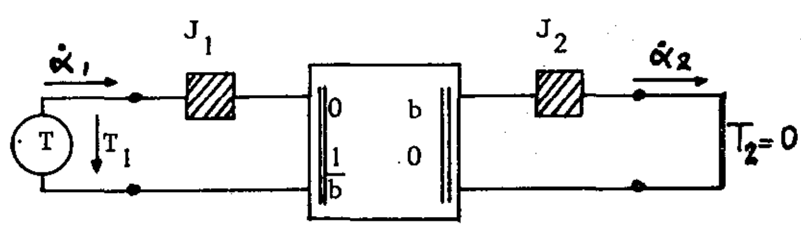

Fig. 2.2.-4. Torque generator connected to the input.

Let $\dot{\alpha}$ and T be sinusoidally varying state magnitudes:

$$\left.\begin{aligned} \dot{\alpha} &= \hat{\dot{\alpha}}.\cos(\omega t + \phi_{\dot{\alpha}}) \\ T &= \hat{T}.\cos(\omega t + \phi_T). \end{aligned}\right\} \quad 2.2.\text{-}(5)$$

The torque generator then will be loaded by an impedance $j\omega J_1$ plus the impedance of J_2 transformed (gyrated) to the input. The magnitude of this gyrated impedance can be determined by using eq. 2.2.-(3) as follows:

$$Z_1 = \frac{T_1}{\dot{\alpha}_1} = \frac{b.\dot{\alpha}_2}{\frac{1}{b}.T_2} = \frac{b^2}{Z_2} \qquad 2.2.\text{-}(6)$$

If

$$Z_2 = j\omega J_2 \qquad 2.2.\text{-}(7)$$

then

$$Z_1' = \frac{1}{j\omega(J_2/b^2)} \qquad 2.2.\text{-}(8)$$

The gyrated impedance thus resembles a rotatory compliance

$$\hat{B} = J_2/b^2 \qquad 2.2.\text{-}(9)$$

Just as with the well-known electrical gyrator (FELDTKELLER), here too, "gyration" produces the dual counterpart of the respective circuitry, thus making impedances to admittances and parallel circuits to series circuits and vice versa. We can thus project J_2 through the two-port to the input, and that yields the following circuit:

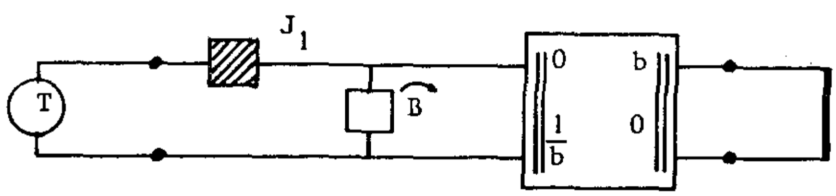

Fig. 2.2.-5. J_2 gyrated to the input.

The short circuit now left parallel to the output can be gyrated to an infinite impedance in series with the input so that we get:

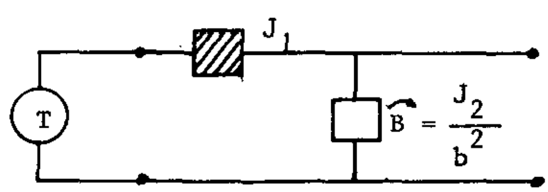

Fig. 2.2.-6. The short circuit at the output becomes an infinite impedance at the input, and the gyrator can be omitted.

The mechanism of nutation

To demonstrate the usefulness of the two-port model of the spinning rotor we can derive the formula for its nutation frequency.

If the gyro spin axis is free to move in all directions - freedom for small angular excursions is sufficient - we can replace the torque generator of fig. 2.2.-6 by a short circuit, thereby obtaining a resonant circuit:

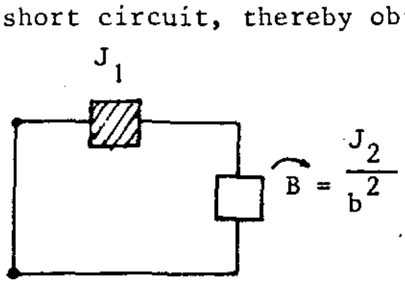

Fig. 2.2.-7. The nutation circuit.

A puls injected into this circuit will make it resonate with the frequency

$$\omega_N = \frac{1}{\sqrt{J_1 . \hat{B}}} = \frac{b}{\sqrt{J_1 \ J_2}} . \qquad 2.2.-(10)$$

This we call the nutation frequency.

It is also possible to grasp the kinematics of the nutation phenomenon by the following consideration using the two-port model:-

Torque and angular velocity of the sinusoidally moving rotation mass J_1 are 90^o out of phase with each other. Since the transducer two-port turns the input torque into an output angular rate this output rate too will be 90^o out of phase with the input rate:

$$\left.\begin{aligned} &\measuredangle\, T_{J_1} \ \dot{\alpha}_{J_1} = 90^o \\ &\measuredangle\, T_{J_1} = \measuredangle\, \dot{\alpha}_2 \end{aligned}\right\} \quad 2.2.-(11)$$

thus $\measuredangle\, \dot{\alpha}_2 \ \dot{\alpha}_{J_1} = 90^o$ and $\alpha_2 \alpha_1 = 90^o$ 2.2.-(12)

If one studies this result at the hand of fig. 2.2.-1 it will be seen that the point of vector $\bar{b}$ describes a kind of Lissajous figure. With $J_1 = J_2$ this will be a circle, with $J_1 \neq J_2$ (unequal moments of inertia of the gimbals) an ellipse.

Rate gyro and rate integrating gyro

The two-port model also allows the study of phenomena that do not strictly belong to the transient class provided the input and output axes and the associated torques and angular velocities can be regarded as orthogonal to each other. To show this use of the model the two main kinds of single degree of freedom gyros shall be taken:-

A rate gyro is obtained by measuring the output torque T_2 that arises from an input angular rate $\dot{\alpha}_1$. The model of the fundamental ideal rate gyro looks like this:

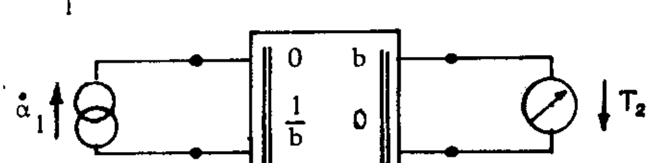

Fig. 2.2.-8. Angular rate source, ideal gyratoric transducer, and torque-meter with infinite input impedance constitute the idealized rate gyro.

The torque-meter can be compared with an electrical voltage meter with very high input impedance. Practically speaking, however, the torque meter impedance is to be represented by a spring (electrically this would be a condensor), the output torque and thus the input angular rate being determined by the spring excursion.

Whereas the rate gyro can be conceived of as a two-port connected to an infinitely high load impedance, the rate integrating gyro will always have a finite secondary load resistor. It forces T_2 and $\dot{\alpha}_2$ to remain in phase at all times. This in turn makes also T_1 and $\dot{\alpha}_1$ in phase with each other and with T_2 and $\dot{\alpha}_2$. Let $\widehat{W}$ represent the rotation resistance at the output axis. We then can write:

$$\frac{T_2}{\dot{\alpha}_2} = \widehat{W} \qquad 2.2.-(13)$$

and with eq. 2.2.-(3)

$$T_2 = b\dot{\alpha}_1 = \widehat{W}\dot{\alpha}_2 \qquad 2.2.-(14)$$

so that

$$\dot{\alpha}_1 = \frac{\widehat{W}}{b}\,\dot{\alpha}_2 \qquad 2.2.-(15)$$

and finally

$$\alpha_1 = \frac{\widehat{W}}{b}\,\alpha_2, \qquad 2.2.-(16)$$

which means that the input angular excursion with respect to inertial space can be measured by the output angular excursion with respect to the orientation of the input axis (compare fig. 2.2.-1), the transfer ratio being determined by $\widehat{W}$ and b.

Validity of the two-port model

The two-port model explained in the foregoing paragraphs allows us to calculate the dynamical behaviour of a spinning rotor gyro (i.e. its response to transients) as well as its response to certain types of steady state signals with the same ease and precision as with any other linear system - provided the input, output, and spin axes sufficiently keep to the orthogonality requirements. Violation of these requirements entails non-linearity, but fundamentally even then the model remains applicable.

3. References

DEIMEL, R.F.; Mechanics of the Gyroscope.
2nd ed., Dover Publications, New York, 1952.

FELDTKELLER, R.; Einführung in die Vierpoltheorie der Nachrichtentechnik.
8.Aufl., Hirzel, Stuttgart, 1962, p. 172.

MAGNUS, K.; Kreisel: Theorie und Anwendungen.
Springer, Berlin, 1971.

PITMAN, G.R.jr. (edit.); Inertial Guidance.
Wiley, New York etc., 1962.

SAVET, P.H. (edit.); Gyroscopes: Theory and Design.
McGraw-Hill, New York etc., 1961.

EINDHOVEN UNIVERSITY OF TECHNOLOGY
THE NETHERLANDS
DEPARTMENT OF ELECTRICAL ENGINEERING

TH-Reports:

1. Dijk, J., M. Jeuken and E.J. Maanders
   AN ANTENNA FOR A SATELLITE COMMUNICATION GROUND STATION (PROVISIONAL ELECTRICAL DESIGN). TH-report 60-E-01. March 1968. ISBN 90 6144 001 7.
2. Veefkind, A., J.H. Blom and L.H.Th. Rietjens
   THEORETICAL AND EXPERIMENTAL INVESTIGATION OF A NON-EQUILIBRIUM PLASMA IN A MHD CHANNEL. TH-report 68-E-2. March 1968. ISBN 90 6144 002 5.
   Submitted to the Symposium on a Magnetohydrodynamic Electrical Power Generation, Warsaw, Poland, 24-30 July, 1968.
3. Boom, A.J.W. van den and J.H.A.M. Melis
   A COMPARISON OF SOME PROCESS PARAMETER ESTIMATING SCHEMES.
   TH-report 68-E-03. September 1968. ISBN 90 6144 003 3.
4. Eykhoff, P., P.J.M. Ophey, J. Severs and J.O.M. Oome.
   AN ELECTROLYTIC TANK FOR INSTRUCTIONAL PURPOSES REPRESENTING THE COMPLEX-FREQUENCY PLANE. TH-report 68-E-04. September 1968. ISBN 90 6144 004 1.
5. Vermij, L. and J.E. Daalder
   ENERGY BALANCE OF FUSING SILVER WIRES SURROUNDED BY AIR.
   TH-report 68-E-05. November 1968. ISBN 90 6144 005 X.
6. Houben, J.W.M.A. and P. Massee
   MHD POWER CONVERSION EMPLOYING LIQUID METALS.
   TH-Report 69-E-06. February 1969. ISBN 90 6144 006 8.
7. Heuvel, W.M.C. van den and W.F.J. Kersten
   VOLTAGE MEASUREMENT IN CURRENT ZERO INVESTIGATIONS.
   TH-Report 69-E-07. September 1969. ISBN 90 6144 007 6.
8. Vermij, L.
   SELECTED BIBLIOGRAPHY OF FUSES.
   TH-Report 69-E-08. September 1969. ISBN 90 6144 008 4.
9. Westenberg, J.Z.
   SOME IDENTIFICATION SCHEMES FOR NON-LINEAR NOISY PROCESSES.
   TH-Report 69-E-09. December 1969. ISBN 90 6144 009 2.
10. Koop, H.E.M., J. Dijk and E.J. Maanders
    ON CONICAL HORN ANTENNAS.
    TH-Report 70-E-10. February 1970. ISBN 90 6144 010 6.

11. Veefkind, A.
NON-EQUILIBRIUM PHENOMENA IN A DISC-SHAPED MAGNETOHYDRODYNAMIC GENERATOR.
TH-Report 70-E-11. March 1970. ISBN 90 6144 011 4.
12. Jansen, J.K.M., M.E.J. Jeuken and C.W. Lambrechtse
THE SCALAR FEED.
TH-Report 70-E-12. December 1969. ISBN 90 6144 012 2
13. Teuling, D.J.A.
ELECTRONIC IMAGE MOTION COMPENSATION IN A PORTABLE TELEVISION CAMERA.
TH-Report 70-E-13. 1970. ISBN 90 6144 013 0.
14. Lorencin, M.
AUTOMATIC METEOR REFLECTIONS RECORDING EQUIPMENT.
TH-Report 70-E-14. November 1970. ISBN 90 6144 014 9.
15. Smets, A.J.
THE INSTRUMENTAL VARIABLE METHOD AND RELATED IDENTIFICATION SCHEMES.
TH-Report 70-E-15. November 1970. ISBN 90 6144 015 7.
16. White, Jr., R.C.
A SURVEY OF RANDOM METHODS FOR PARAMETER OPTIMIZATION.
TH-Report 70-E-16. February 1971. ISBN 90 6144 016 5.
17. Talmon, J.L.
APPROXIMATED GAUSS-MARKOV ESTIMATORS AND RELATED SCHEMES.
TH-Report 71-E-17. February 1971. ISBN 90 6144 017 3.
18. Kalášek, V.
MEASUREMENT OF TIME CONSTANTS ON CASCADE D.C. ARC IN NITROGEN.
TH-Report 71-E-18. February 1971. ISBN 90 6144 018 1.
19. Hosselet, L.M.L.F.
OZONBILDUNG MITTELS ELEKTRISCHER ENTLADUNGEN.
TH-report 71-E-19. March 1971. ISBN 90 6144 019 X.
20. Arts, M.G.J.
ON THÉ INSTANTANEOUS MEASUREMENT OF BLOODFLOW BY ULTRASONIC MEANS.
TH-Report 71-E-20. May 1971. ISBN 90 6144 020 3.
21. Roer, Th.G. van de
NON-ISO THERMAL ANALYSIS OF CARRIER WAVES IN A SEMICONDUCTOR.
TH-Report 71-E-21. August 1971. ISBN 90 6144 021 1.
22. Jeuken, P.J., C. Huber and C.E. Mulders
SENSING INERTIAL ROTATION WITH TUNING FORKS.
TH-Report 71-E-22. September 1971. ISBN 90 6144 022 X.

23. Dijk, J. and E.J. Maanders
APERTURE BLOCKING IN CASSEGRAIN ANTENNA SYSTEMS. A REVIEW.
TH-Report 71-E-23. September 1971. ISBN 90 6144 023 8 (in preparation).
24. Kregting, J. and R.C. White, Jr.
ADAPTIVE RANDOM SEARCH.
TH-Report 71-E-24. October 1971. ISBN 90 6144 024 6 (in preparation).
25. Damen, A.A.H. and H.A.L. Piceni
TH-Report 71-E-25. October 1971. ISBN 90 6144 025 4 (in preparation).
26. Bremmer, H.
A MATHEMATICAL THEORY CONNECTING SCATTERING AND DIFFRACTION PHENOMENA, INCLUDING BRAGG-TYPE INTERFERENCES.
TH-Report 71-E-26. December 1971. ISBN 90 6144 026 2.
27. Bokhoven, W.M.G. van
METHODS AND ASPECTS OF ACTIVE-RC FILTERS SYNTHESIS.
TH-Report 71-E-27. 10 December 1970. ISBN 90 6144 027 0.
28. Boeschoten, F.
TWO FLUIDS MODEL REEXAMINED.
TH-Report 72-E-28. March 1972. ISBN 90 6144 028 9.
29. Rietjens, L.H.Th.
REPORT ON THE CLOSED CYCLE MHD SPECIALIST MEETING. WORKING GROUP OF THE JOINT ENEA:IAEA INTERNATIONAL MHD LIAISON GROUP AT EINDHOVEN, THE NETHERLANDS. September 20, 21 and 22, 1971.
TH-Report 72-E-29. April 1972. ISBN 90 6144 029 7
30. C.G.M. van Kessel and J.W.M.A. Houben
LOSS MECHANISMS IN AN MHD-GENERATOR.
TH-Report 72-E-30. June 1972. ISBN 90 6144 030 0.
31. A. Veefkind
CONDUCTING GUIDS TO STABILIZE MHD-GENERATOR PLASMAS AGAINST TONIZATION INSTABILITIES. TH-Report 72-E-31. October 1972. ISBN 90 6144 031 9.
32. J.E. Daalder and C.W.M. Vos
DISTRIBUTION FUNCTIONS OF THE SPOT-DIAMETER FOR SINGLE- AND MULTI-CATHODE DISCHARGES IN VACUUM. TH-Report 73-E-32. January 1973. ISBN 90 6144 032 7.
33. J.E. Daalder
JOULE HEATING AND DIAMETER OF THE CATHODE SPOT IN A VACUUM ARC.
TH-Report 73-E-33. January 1973. ISBN 90 6144 033 5.